



3D model generated from UAV photogrammetry and semi-automated rock mass characterization

María J. Herrero^{a,*}, A. Patricia Pérez-Fortes^b, José I. Escayó^c, Juan M. Insua-Arévalo^d, Raúl De la Horra^d, Francisco López-Acevedo^a, Laura Trigos^c

^a Departamento de Mineralogía y Petrología, Facultad de Geología, Universidad Complutense de Madrid, 28040, Madrid, Spain

^b Departamento de Ingeniería Civil: Construcción, ETSICCP, Universidad Politécnica de Madrid, Spain

^c Departamento de Ingeniería y Morfología del Terreno, ETSICCP, Universidad Politécnica de Madrid, Spain

^d Departamento de Geodinámica, Estratigrafía y Paleontología, Facultad de CC. Geológicas, Universidad Complutense de Madrid, Spain

ARTICLE INFO

Keywords:

UAV
3D models
Photogrammetry
Semi-automated rock-mass characterization

ABSTRACT

This work develops a rock mass characterization of a limestone quarry in northern Spain based on a 3D model obtained by using photographs taken from an unmanned aerial vehicle (UAV) flight and structure-from-motion algorithms. This methodology permits to obtain photogrammetric information in a rapid and low-cost way.

Geological planar facets (stratification, faults) are related to the tectonic history of a geological formation and permit assessing slope stability. The spatial orientation of planar features is usually measured with a compass and clinometer, which requires experience and knowledge, it is space limited, and sometimes hazardous. Geological 3D models can mitigate these limitations. A 3D point cloud generated from a series of images obtained using an UAV is included in the open-access applications DSE and FACET, which serve to determine the main discontinuity planes within a limestone quarry. Comparison of the results from software analyses with data hand-measured directly in the field reveals the effectiveness of the use of UAV to develop a virtual outcrop model that permits to obtain accurate measurements. The resultant quarry 3D model has been included in Sketchfab, an open access platform that permits easy and quick access and availability for a wide audience.

This study shows that the use of UAV combined with structure-from-motion algorithms is of great interest for geosciences as well as other related disciplines such as mining or civil engineering, and can facilitate decision-making for policy makers and authorities. In addition, it is a technique of great use to develop rock mass characterization in a low-cost, rapid, and easy way, and permits to reach areas with difficult accessibility. This way, this methodology can also be very useful for geosciences teaching purposes, as a complement to traditional field lectures, or to develop virtual field trips and laboratories.

1. Introduction

Discontinuities are essential elements that affect slopes stability, the rock mass strength, and permeability (Hudson, 2001; Brown and Hoek, 1980). There are several geomechanical classifications (Barton, 1978; Bieniawski, 1989; Romana, 1985; Hack et al., 2003; Pantelidis, 2009; Tomás et al., 2012), and for all of them a detailed characterization of discontinuities and their properties is critical, being necessary to define parameters such as orientation, spacing, persistence, roughness, and aperture among others (Wang et al., 2003). Traditionally, surveys and studies of rock mass characterization were made by direct measurements of the spatial distribution of discontinuity planes (i.e., joints,

faults, bed plane, foliations), which requires understanding the discontinuity sets that affect the outcrops. The analysis has to be defined by measuring the orientation (dip and dip direction) of many discontinuities, their spacing, and persistence, and translating these data into stereographic plots where the main discontinuity sets are determined based on pole density distributions. Once every set is identified, a statistical analysis is developed to determine their representative spacing and persistence. This approach is time-consuming, difficult to apply in places of dangerous or impossible access, and depends on the accuracy and the ability of the geologist or engineering geologist to take proper measurements. Thus, the use of alternative safe and fast surveying technologies improves the quality of the results. The International

* Corresponding author.

E-mail address: mjherrer@ucm.es (M.J. Herrero).

<https://doi.org/10.1016/j.cageo.2022.105121>

Received 30 August 2021; Received in revised form 15 December 2021; Accepted 25 April 2022

Available online 29 April 2022

0098-3004/© 2022 The Authors. Published by Elsevier Ltd. This is an open access article under the CC BY license (<http://creativecommons.org/licenses/by/4.0/>).

Society for Rock Mechanics (Barton, 1978) recommended photogrammetry to measure discontinuity, and recent advances have led to numerous studies developing semi-automated extraction and characterization of discontinuities based on analyses of 3D point clouds, commonly used in non-contact surveys such as Laser Imaging or LiDAR (Slob et al., 2005; Kemeny et al., 2006; Mah et al., 2011; Maerz et al., 2013; Deliormanli et al., 2014; Riquelme et al., 2015; Chen et al., 2016; Jianqin et al., 2016; Jordá Bordehore et al., 2017; Drews et al., 2018).

Similarly, Unmanned Aerial Vehicle (UAV) photogrammetry appears as a method that offers a viable cost-effective alternative to traditional remote sensing systems such as laser scanners, photogrammetry from airplanes, or satellite imagery, (Barton, 1978) especially for analyzing small areas. The use of UAV allows rapid acquisition of high-resolution photographs from airborne cameras (Wang et al., 2020). Giordan et al. (2015) proposed UAV data acquisition and processing methods to monitor active small landslides affecting urban environments; Bonali et al. (2019) analyzed evidence of tectonic and volcano-tectonic activity in the Iceland rift, and DeBell et al. (2016) reviewed the use of UAVs to manage water resources; UAV techniques are also relevant in the analysis of geological hazards (Tu et al., 2021), and this technology appears as a safe and fast monitoring technique for geotechnical, geological, and other engineering applications, such as the estimation of errors in position or volume uncertainties in civil engineering projects (ie. quarries, roads, etc. Siebert and Teizer, 2014; Castiglioni et al., 2017; Tziavou et al., 2018) and the determination of variations of stockpile volumes in quarries (Raeva et al., 2016). Photogrammetry developed with information obtained from UAV has been used as well in previous works to create high resolution terrain models that are important sources of geographical and geological information for disciplines related to Geosciences (Ouédraogo et al., 2014; Vasuki et al., 2014; Madden et al., 2015), and to obtain terrain features (with cm accuracy) or to create 3D models from high resolution point clouds (Labourdette and Jones, 2007; James and Robson, 2012; García-López et al., 2018).

Additionally, outcropping planes represent a wide variety and geologically relevant features: sedimentation mechanisms, tectonic events, etc. In 3D environments and point clouds, planes appear as a rock geometrical feature that is easy to define. Planes are the simplest 3D geometric item, and currently there are many studies looking for methods to obtain them automatically (Riquelme et al., 2014; Vasuki et al., 2014; Dewez et al., 2016; Jianqin et al., 2016; Jordá Bordehore et al., 2017).

The present work investigates the utility of using UAVs as a tool to generate an outcrop 3D model that provides a 3D point cloud of the terrain surface from which a rock mass characterization is developed by

semi-automated extraction of discontinuities (Deb et al., 2008; Sturzenegger and Stead, 2009; Menegoni et al., 2019; Giordan, D. et al., 2020; Buyer et al., 2020; Kong et al., 2021). Mechanical characterization has been performed using a photogrammetric analysis in a limestone quarry in northern Spain, where every year students of the degree of Engineering Geology develop a field trip to learn about geological mapping cartography and rock mass characterization (Fig. 1). The UAV survey covers a 65 m long and 30 m high quarry bench. A multi-rotor DJI Phantom 3© equipped with a digital camera was used to survey the rock outcrop. Data acquisition took approximately 20 min, and point cloud creation took 6 h. The reconstruction of the camera positions, the generation of a high-resolution point cloud, the 3D model, and the determination of different surface characteristics were obtained using Structure from Motion (SfM, AGISOFT PhotoScan LLC, 2014) computer vision techniques in multi-view photos with cm accuracy (Verhoeven, 2011; Westoby et al., 2012). The generated 3D point cloud was processed by the open-access software CloudCompare (Girardeau-Montaut, 2016), and discontinuities were extracted by the open software DSE (Discontinuity Set Extractor (Riquelme et al., 2014) and FACETS (Dewez et al., 2016). Finally, the results obtained from both software have been compared with data measured directly in the field during fieldwork campaigns by teachers and undergraduate students at University Geology Degrees.

2. Geological setting and aerial photographs

The analyzed outcrop is located within the Cantabrian Zone (Lotze, 1945), in northern Spain (Fig. 1a), which forms the western part of the European Variscan belt (Marcos and Pulgar, 1982; Gallastegui et al., 1997). This area belongs to a thin-skinned foreland thrust and fold belt (Julivert, 1978; Pérez-Estaún et al., 1988), characterized by a folded and fractured thick sedimentary paleozoic unit (Fig. 1b). The paleozoic succession consists of cambrian limestones and sandstones, followed upsection by ordovician and devonian quartzarenites and a carboniferous sequence of siliciclastic layers alternating with carbonate units on top (Aller, 1986). The Alpine North to South compression produced a thrust fault, and Variscan structures were reactivated and uplifted in the Bay of Biscay to the north and the Duero basin to the south (Alonso and Pulgar, 1993). Abundant veins and dikes indicate the existence of hydrothermal activity related to rift extensional events produced during the North-Atlantic opening, and appear related to Mississippi Valley Type mineralization (Sánchez et al., 2009).

The outcrop at which the rock mass characterization is performed is one of the benches of an open pit quarry in the Barcaliente Fm

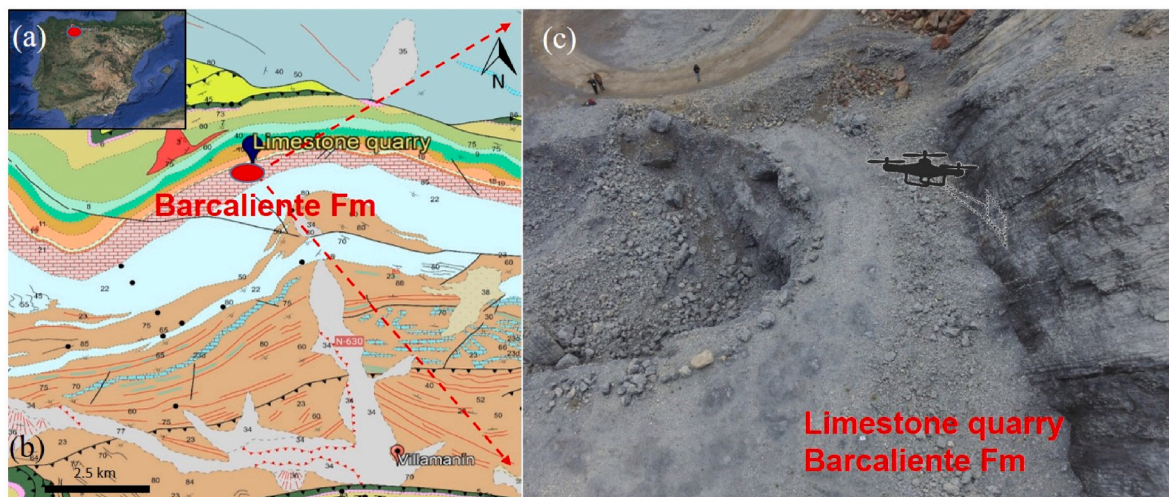


Fig. 1. Study area: (a) Location of the study area in northern Spain; (b) Geological map of the area with the location of the limestone quarry within the Barcaliente Formation, to the north of the village of Villamanín, León (Spain). (c) Image of the outcrop at which the UAV survey has been carried out.

(Carboniferous in age), made up of greyish black, and well-bedded micritic limestones (Fig. 1c). In the outcrop, the strata, with centimeter to decimeter thickness, appears subvertical, slightly overturned, and presenting a NNW dipping. The fracture network results from the interaction of both orogenies, the Variscan and the Alpine. Therefore, this outcrop is interesting for teaching purposes due to the geological complexity of the area, which can be easily and clearly analyzed in the limestone quarry. A substantial part of the study area is inaccessible due to its height, which exceeds 30 m. To allow visualization of the quarry, it has been pictured using a UAV. Photogrammetric information has been used to 3D model the geological structure of the rock mass.

3. Methodology

Characterization and classification of rock discontinuities allow determining parameters such as the strength or permeability of rock masses as well as establishing the stability of surface and under-ground excavations (Brown and Hoek, 1980; Hudson, 2001). In this study, a quarry has been analyzed in detail by conducting several fieldwork campaigns, composed of 4 compass scanlines. A UAV flight has been performed in the same quarry to obtain a photograph dataset that has led to the development of a 3D model and establish a discontinuities analysis with two open access software such as DSE and FACETS. The results are finally compared with data obtained by direct measurements in the field. Therefore, by developing this type of analysis for teaching purposes, students learn both techniques, how to measure data in the field, and the use of different software packages (Fig. 2) and interpret and compare results.

3.1. Acquisition of photographs of the outcrop: UAV flight planning

Data acquisition in this study consists of georeferenced aerial photographs obtained from a DJI Phantom 3© UAV flight. The UAV has four

blades and is equipped with an intelligent flight battery, remote controller, camera, and a stereo Vision Positioning System (VPS). The former allows to fly safely even without satellite positioning (Yusoff et al., 2018). The digital camera mounted on the UAV was a Nikon D3200 mounted with a 28 mm lens, with a resolution of 12.4 megapixels.

Once in the air, the aircraft is programmed to automatically fly a grid pattern horizontally over the outcrop (autopilot mode), and takeoffs and landings were conducted by a licensed pilot from the ground. The UAV camera took a photograph every 1–2 s. Synchronization of the flight path with the camera was made before the flight using PIX4D© software (Pix 4D mapper, 2018). The flight of the aircraft was previously defined in detail, including flight altitude, speed, number of strips, and overlap of the photographs. The resolution per pixel of the pictures was 5 cm.

The flight was conducted in six horizontal stripes, spaced approximately 10 m apart, resulting in 80% and 60% forward and side overlaps, respectively. This level of overlap is enough to generate accurate 3D models (AGISOFT PhotoScan LLC, 2014), at an elevation of 50 m above the terrain. The UAV survey was completed in 10 min (it was repeated several times) for the 4000 m² study area and the 65 m long quarry.

3.2. Determination of camera locations and production of the sparse point cloud

Photographs taken from the UAV were processed using the Structure from Motion (SfM) methodology, from which the 3D structure is generated from overlapping images (Blistan et al., 2016). Structure from Motion (SfM) was developed with the AGISOFT PhotoScan Professional Version 1.1 software environment (AGISOFT PhotoScan LLC, 2014). The program can determine the camera positions (Fig. 3) and ground characteristics by identifying and matching different features from the available photographs. In total, 77 images were used to create the sparse point cloud, resulting in 15767 points after 6 h of processing. Afterwards, a dense point cloud of 1188361 points was generated, with a resolution of 1.25 cm and the textured mesh containing the ground features (Fig. 4).

This 3D mesh was produced by the Poisson Surface Results (Nesbit et al., 2020), and the resulting information was then included as the graphical framework for geological structures (fault planes and other discontinuities) recognition. Finally, the open-source software CloudCompare (Girardeau-Montaut, 2016) was also used for 3D visualization and computation.

3.3. Discontinuity Set Extractor (DSE)

The dense point cloud dataset obtained by the SfM approach has been used to perform a Discontinuity Set Extractor (DSE) statistical analysis of the data. DSE is an open software based on MATLAB and designed by the University of Alicante in Spain (Riquelme et al., 2014). The software detects structural discontinuities of rock masses from 3D point clouds that are generated with field data obtained from remote sensing methods and photogrammetry. Discontinuities are ordered in sets that define a plane, and similar planes constitute discontinuity clusters. Thus, the software detects different point sets and characterizes the clusters of discontinuities present in a rock mass by performing the following operations:

- 1) Local curvature calculation: DSE finds the discontinuities' orientation of the rock mass at every point of the 3D point cloud. Simultaneously, the software detects the k-nearest neighbors (knn) or nearest points to each data analyzed with the same orientation, creating sets of points. Riquelme et al. (2014) suggest ranging the knn parameter between 15 and 30, with the highest value being the most effective. Once the sets of points have been defined, DSE develops a coplanarity test to group each point of the 3D point cloud and their corresponding nearest neighbors into planes. Rencher

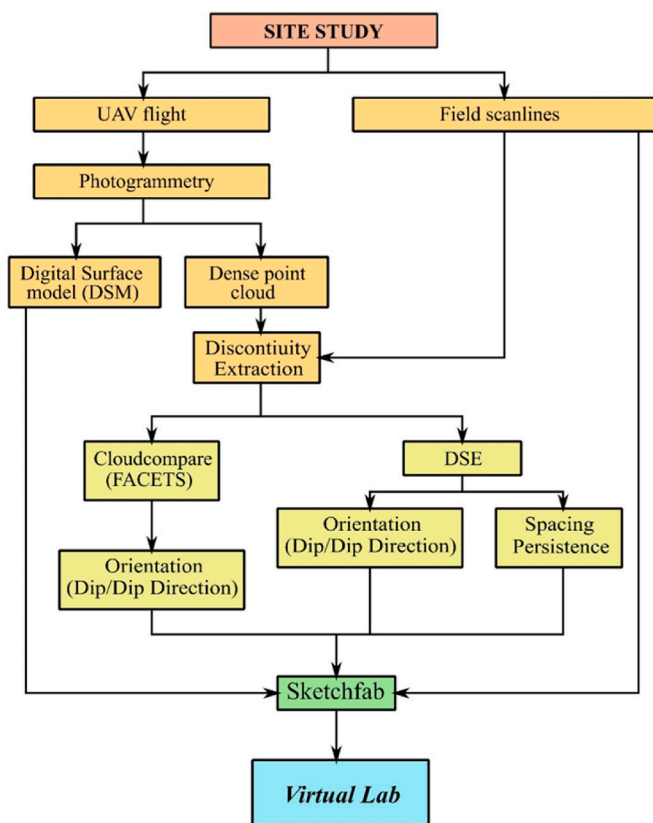


Fig. 2. Workflow of the data processing chain of this study.

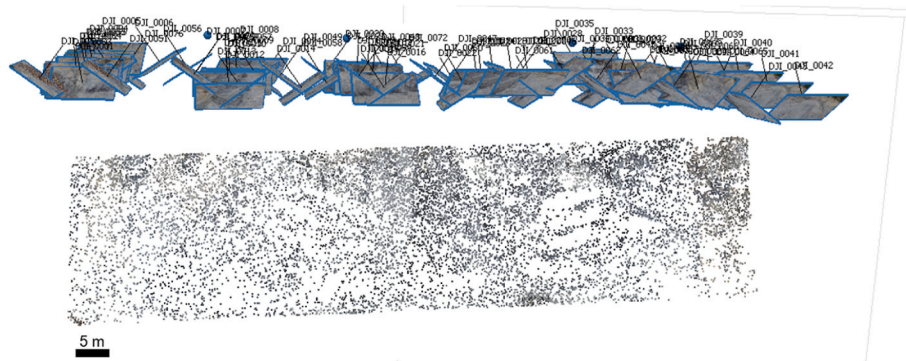


Fig. 3. Sparse point cloud generated by SfM pipeline from AGISOFT PhotoScan (2014).



Fig. 4. Mesh and 3D model of the quarry surface from AGISOFT PhotoScan, 2014.

(2012) proposes that the admissible variance or deviation in the orientation of the forming points of a set is 80%. Therefore, the tolerance value of the coplanarity test (η_{\max}) is commonly set as 20%. Thus, this 20% tolerance has been applied. Finally, DSE determines the best-fit plane for the point sets previously generated and calculates the normal vector for this plane. The operator defines the minimum deviation angle between the normal vectors of the sets of points and the principal vector of the best-fit plane (Angle min v ppal) to group different sets into planes (Riquelme et al., 2014, 2016).

- 2) Statistical analysis of the planes: DSE projects the poles of the discontinuity planes or normal vectors previously defined in a density stereographic plot by using the Kernel density estimation KDE method (Silverman, 1986). In the resultant plot, the software locates the areas with maximum pole densities and assesses the clusters of discontinuities, applying two parameters controlled by the user, the cone filter angle and the maximum number of clusters (np). The cone filter angle is the minimum accepted distance between two poles of planes of discontinuities, to consider that these planes belong to a cluster. The maximum number of clusters is established by the user, and it depends on the number of discontinuities present in the rock mass previously observed in direct field observations (Riquelme et al., 2014, 2015; Jordá Bordehore et al., 2017).
- 3) Cluster analysis: DSE characterizes discontinuity clusters by assessing their main pole dip and dip direction. It is possible to hand-edit the final number of clusters regarding the number of points per cluster (ppc). Riquelme et al. (2014) state that clusters with less than 100 points can be statistically considered as noise in the model.
- 4) Normal and persistence calculations: Once the software has detected the different clusters in the model, it can assess the spacing and persistence of the different discontinuity sets present in the model.

Therefore, the advantage of using DSE relays in the possibility of obtaining a substantial number of virtual compass measurements in a

short period of time (Riquelme et al., 2014).

3.4. FACETS

FACETS is an open plugin from CloudCompare software that extracts planar facets from 3D point clouds, calculates their dip and direction, and plots them in stereograms. To extract the planar facets from the model, the software segments the dense cloud of points in facets with a user-defined degree of coplanarity using two algorithms, the kd-tree method (KD) or the fast-marching method (FM) (Dewez et al., 2016). The KD algorithm covers the 3D model by a lattice of cells obtained by repeatedly splitting the 3D point cloud into smaller flat patches, until these patches coincide with one of the best-fitting faces obtained by the Root Mean Square (RMS) threshold (maximum distance). In contrast, the FM algorithm divides the 3D point cloud into smaller patches that are regrouped. Hence, the patches will have similar sizes and will be equal or larger than a pixel (Dewez et al., 2016). Due to the geological complexity of the outcrop and the amount and type of discontinuities present in the analyzed quarry, the method selected in this paper is the KD algorithm.

After the KD analysis and segmentation of the point cloud into coplanar elementary subdivisions, the software performs three different levels of clustering. At a first level, FACETS clusters the elementary subdivisions that belong to a small fragment of a plane. At a second clustering level, elementary planes are grouped into single planes that belong to the same overall plane. Finally, at a third clustering level, parallel planes are combined into plane sets sharing the same spatial attitude (Dewez et al., 2016).

3.5. Field measurements

Every year, undergraduate students of the 4th year Engineering Geology Degree from the Complutense University of Madrid (Spain) visit the area to study the structural geology and develop a rock mass

characterization analysis. For this purpose, teachers and students perform several scanlines with their compass in the studied outcrop (Barton, 1978).

Due to the limited accessibility to the quarry face, in this work, teachers and students performed four scanlines with 15 m of length and covering a height of up to 2 m during the 2018/2019 course. In addition to orientation measurements, spacing and persistence data were collected with a measure tape along the 4 scanlines.

3.6. Platform for dissemination: web-based 3D mesh (sketchfab)

Virtual outcrops (VO) and Digital Outcrop Models (DOM) provide photorealistic models for geosciences with high spatial precision and characteristics such as geometric relationships between geologic features can be easily observed Bellian et al. (2005); Jones et al. (2009); Herrero Fernández et al., 2019; Sánchez Moya et al., 2020.

The generation of 3D outcrop models has greatly evolved during the last few years due to recent technological advances. Commonly, these models appear as large file sizes and the need for 3D programs (some requiring payment for their use), with difficulties in sharing and visualizing them. Within this context, there are platforms for model dissemination, such as Sketchfab (2020), which can be used either to improve students learning or to share results and interpretations in an intuitive and visually attractive environment (Nesbit et al., 2020), and even to obtain additional measurements from areas with dangerous, difficult, or impossible access, where traditional methods are inadvisable.

4. Results

The development of the DSE analysis, performed following up the steps defined in section 3.4, has led to identification of four discontinuity clusters (Fig. 5 and Table 1).

In addition, the main discontinuities extracted by FACETS (section 3.5) are shown in Fig. 6 and Table 2 (see Fig. 7).

Finally, field measurements reveal the existence of seven sets or discontinuity families (S1–S7, Table 3). Sets 2 to 6 are fractures related to the different tectonic events that occurred in the area, while set 7 corresponds to the stratification of the limestones. Set 1 is the main fracture set, which is vertical to subvertical, close to the stratification dip.

4.1. Comparison between field measurements and DSE and FACETS results

The results obtained by the measurements of the compass scanlines have been compared with the discontinuities extracted from the 3D point cloud obtained from the UAV photographs using DSE and FACETS software (Table 4). In the three applied methods, it is considered that a

plane belongs to a discontinuity set if its dispersion is $\leq 30^\circ$ with respect to the mean plane of the set. Thus, the clusters have been grouped and correlated according to this admissible dispersion (Table 4).

It is observed that the DSE software has detected and calculated the orientation and properties of 2 sets (S3 and S6; Table 4). FACETS software has extracted and detected sets similar to S1, S2, S3, and S6 obtained from measurements in the outcrop (Table 4). It is noticeable that neither of the two software has been able to detect the stratification of the limestone (S7) or the joints S4 and S5, which are subvertical and perpendicularly oriented to the model. Therefore, their surfaces are reduced to lines that are not automatically extracted using these types of extraction methods. Depending on the orientation of the planes and the position from which the photographs are taken, the planes of a rock mass discontinuities can be observed as surfaces or traces and are not extracted. Both programs are only able to extract planes from surfaces in the 3D model.

The comparison of the planes obtained from field measurements, and the planes obtained by the DSE and FACETS software analyses lead to the identification of one plane that is coincident in the three methods, S6, J4, and F4 (Table 4). The orientation of the quarry face analyzed has been detected by both software (S3, J1 and F1, Table 4). On the contrary, FACETS has detected three planes identified in the field as well (S1 and F2; S2 and F3; S6 and F5). It is noticeable, though, that the similarity of hand-measured planes and those obtained with the FACETS software show a more accurate correspondence. Finally, both software has determined new sets that were not measured in the outcrop, named S8 (only DSE) and S9 (both software). These sets could correspond to joint that are inaccessible on the quarry face, and these should be considered in future field campaigns.

The spacing and persistence of the sets measured in the field and by DSE are also shown in Table 5. It can be observed that the spacing measured in the field in sets S1 and S6 is lower than 10 cm. This measurement is lower than the proper resolution of the created model (1 m). Therefore, the spacing obtained from the DSE analyses for the J1 set appears to be of a higher value than the real one, and the same occurs with persistence.

4.2. Limitations of DSE and FACETS semi-automatic analysis in the case of study

High resolution UAV photographs allow the development of 3D outcrop models and the identification of geological features such as stratification, discontinuity planes, or even boundary surfaces. This identification can be improved including additional field data, and permit to reach dangerous places or with difficult access. Limitations arise when trying to generate models in complicated settings: places with complex color backgrounds. In these cases, the result of the software can contain large unwanted areas in the point cloud. To solve this problem, outcrop reconstructions should ensure that the depth of the

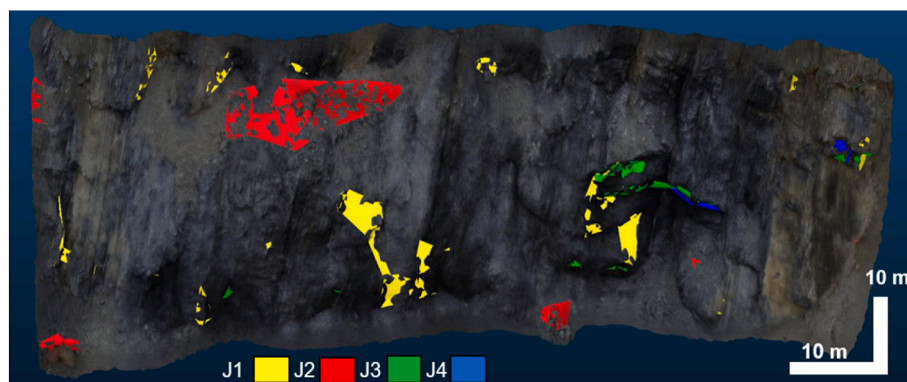


Fig. 5. Results of the discontinuity Set Extractor (DSE) analysis with the resultant main discontinuity clusters, J1, J2, J3 and J4, obtained from the 3D point cloud.

Table 1
Clusters extracted with the DSE Analysis.

Cluster	Dip (°)	Dip Direction (°)	Density (%)	Normal spacing (m)	Persistence (m)	Geological Significance
J1	17	142	10	–	–	Quarry Slope
J2	29	360	0.8	0.89	2.66	Joint
J3	52	122	0.2	1.24	2.15	Joint
J4	75	163	0.2	–	18.34	Joint



Fig. 6. Results of the FACETS analysis with the main discontinuity planes F1, F2, F3, F4, F5 obtained from the 3D point cloud.



Fig. 7. Capture image of the 3D digital outcrop model implemented in the open-access platform for 3D visualization “Sketchfab” (<https://sketchfab.com/3d-models/villamanin-leon-spain-5874116f37964ddc8a62b156847d2330>).

Table 2
Clusters extracted with the FACETS analysis.

Cluster	Dip (°)	Dip Direction (°)	Geological significance
F1	15	165	Quarry Slope
F2	38	95	Joint
F3	21	213	Joint
F4	57	138	Joint
F5	53	176	Joint

photograph field is focused on the outcrop.

Another limitation of the UAV-SfM photogrammetry technique is that it is unable to reconstruct surfaces in the case of studying vegetated or cloudy or shadow areas, while other methods such as LiDAR are able to achieve this. These limitations could be solved by flying during the season with less vegetal cover (i.e., in the summer), or by limiting the presence of shadows by taking the pictures with zenithal light.

Discontinuity semi-automated extractor software such as DSE and FACETS is primarily limited to the orientation of the pictures taken to create the 3D point clouds and the proper discontinuities. Vertical

Table 3
Field measurements of discontinuity planes and their geological significance according to field observations.

Cluster	Dip (°)	Dip Direction (°)	Spacing (m)	Persistence (m)	Geological Significance
S1	61	335	<0.02	<2	Joint
S2	39	245	1	>10	Joint
S3	16	120	–	–	Quarry slope
S4	60	60	2.5	No visible	Joint
S5	50	210	No visible	No visible	Joint
S6	71	170	0.01	2	Joint
S7	88	65	0.01	Continuous	Bed planes

discontinuities, or those perpendicular to the camera, cannot be detected by these methods. Thus, manual analysis of traces in digital images or 3D models, using commercial software such as ShapeMetriX or the compass plugin in CloudCompare (Buyer and Schubert, 2018; Pack et al., 2021) or any other semi-automatic method for trace extraction (Vasuki et al., 2014; Li et al., 2016 or Guo et al., 2019) must be applied.

Table 4

Correspondence of discontinuities detected with FACETS and DSE with the observed in the field.

Field			DSE			FACETS		
Cluster	Dip (°)	Dip direction (°)	Cluster	Dip (°)	Dip direction (°)	Cluster	Dip (°)	Dip direction (°)
S1	61	78				F2	38	95
S2	39	245		–	–	F3	21	213
S3	16	120	J1	17	142	F1	15	165
S4	60	60		–	–		–	–
S5	50	210		–	–		–	–
S6	71	170	J4	75	163	F5	53	176
S7	88	65		–	–		–	–
S8	–	–	J2	29	360		–	–
S9	–	–	J3	52	122	F4	57	138

Table 5

Correspondence of the spacing and persistence of the discontinuities detected with DSE and the ones observed in the field.

Field					DSE				
Cluster	Dip (°)	Dip direction (°)	Spacing (m)	Persistence (m)	Cluster	Dip (°)	Dip direction (°)	Spacing (m)	Persistence (m)
S1	61	78	<0.02	<2					
S2	39	245	1	>10		–	–		
S3	16	120	–	–	J1	17	142	0.71	4.37
S4	60	60	2.5	No visible		–	–		
S5	50	210	No visible	No visible		–	–		
S6	71	170	0.01	2	J4	75	163	–	18.34
S7	88	65	0.01	Continuous		–	–		
S8	–	–	–	–	J2	29	360	0.89	2.66
S9	–	–	–	–	J3	52	122	1.24	2.15

Furthermore, the use of these software requires previous knowledge of the structural geology of the area to assess the correct number of clusters, as well as some knowledge of statistics to properly establish the clustering process. In addition, the data obtained from this study, especially those related to spacing and persistence calculations, are directly limited by the resolution of the model. In the present study, the model was designed for teaching purposes, and georeferenced images from the UAV were considered accurate enough to develop the 3D model and to show students the structure of the rock mass. However, although the accuracy of the model is not high enough to represent the real spacing and persistence of the discontinuities detected, this problem could also occur with more precise models with topography surveys implemented in areas with very close spacing.

Virtual outcrops or 3D outcrop models can become an excellent means of studying terrain properties, although results show greater accuracy by combining them with field visits. The use of this methodology may serve to improve scientific visualizations, helping the analysis of data, increasing the number of field measurements, and providing new visual perspectives, even for teaching purposes of both geology and computing methods.

4.3. Sketchfab web platform for dissemination of the 3D model

This Sketchfab web-based interface permits to upload models and establish different rendering options, include comments, etc. (Fig. 7). There are as well various texture resolutions and Virtual Reality (VR) environment, allowing to extend and amplify the sensory experiences of the user who can get many details and an almost complete immersive experience within the model (<https://sketchfab.com/3d-models/villa-manin-leon-spain-5874116f37964ddc8a62b156847d2330>). Thus, this platform can be of great use to develop future virtual laboratories and field trips for Geosciences students. In addition, this platform can be used as an attractive repository of LiDAR and photogrammetry data as the one proposed by Lato et al. (2013). Sketchfab permits to stick annotations on the models. Annotations are small, clickable notes, which may include images, lines, or explanations. They have a title and description and can be added from the Edit 3DSettings menu on the

platform.

5. Conclusions

The development of 3D outcrop models from UAV outcrop mapping allows obtaining detailed characterization of geological outcrops. The results obtained prove that UAV photogrammetry can be used to identify discontinuities and thus enhance rock mass characterization studies in unreachable areas and seem a valuable solution in terms of safety, accuracy, cost, and efficiency. UAVs are inexpensive devices compared to other techniques for field surveying, and they have proved to be the most suitable source of photogrammetric information for small areas.

Discontinuity semi-automated extractor software are open-access and fast tools that can complement field data acquisition (compass data), especially for limited access outcrops. They can extract the main discontinuity planes and group them into different discontinuity sets with different orientations, providing relevant information of rock mass characterization analyses and improving the existing. DSE is also able to calculate other relevant properties for geomechanical purposes, such as the spacing and persistence of each set of discontinuities detected, although the FACETS results appear more similar to the outcrop data in this study. The resulting 3D models can be of use for teaching rock mass characterization, as well as the use of different software and web-platforms.

Sketchfab and other internet platforms provide a straightforward way to share data sets and 3D models with other scientists, students, and stakeholders with no need of programming or using expensive specialized software. The possibility of implementing the 3D model as a Virtual Reality (VR) environment permits to extend and amplify the sensory experiences of the end-users.

For the moment, 3D models will not replace field surveys because the information obtained by an experienced geologist's eye and by the rest of the senses cannot be replaced. There will appear cases where planar features of interest are not measurable surfaces, and in this case the resulting point clouds will not generate relevant information. In other cases, plane widths would not be sufficiently determined by the point cloud, or inaccurate results would be obtained, for example due to the

wrong selection of the points of view of the survey. The study of virtual outcrops is a worthwhile technique for many applications in geology, although it will not replace fieldwork, but combining geoscientist knowledge with new technology domains will permit establishing future needs to achieve optimization and efficiency.

Code availability section

The open software codes used in this manuscript are available in the following repositories:

Cloudcompare v. 2.10.2. <https://github.com/cloudcompare/cloudcompare>;

FACETS (CloudCompare plugin). http://www.cloudcompare.org/doc/wiki/index.php?title=Facets_%28plugin%29;

DSE v. 3.01. <https://github.com/cloudcompare/cloudcompare>.

3D model and data associated showed in this work are also available in <https://sketchfab.com/3d-models/villamanin-leon-spain-5874116f37964d4c8a62b156847d2330>.

Other commercial tools are available for downloading in their respective websites: Pix 4D mapper from <https://www.pix4d.com/es/and> Sketchfab from <https://sketchfab.com/>.

Authorship contribution statement

María J. Herrero: Conceptualization, investigation, writing, methodology, supervision, software. Patricia Pérez-Fortes: Conceptualization, data curation, methodology, writing. José I. Escavy: Investigation, writing, and visualization. Juan M. Insua-Arévalo: Conceptualization, review. Raúl De la Horra: Investigation, review. Francisco López-Acedo: Software, validation. Laura Trigos: Writing-reviewing and editing.

Declaration of competing interest

The authors declare that they have no known competing financial interests or personal relationships that could have appeared to influence the work reported in this paper.

Acknowledgments

The authors would like to acknowledge Project PID 2019-106887 GB-C33 and Universidad Complutense de Madrid for supporting the study with the Teaching Innovation Project PIMCD-2018-nº24, PIMCD-2019-nº 305, Proyecto Innova Docencia-2020-157 and Proyecto Innova Docencia-2021-278.

References

AGISOFT PhotoScan, L.L.C., 2014. AGISOFT PhotoScan PhotoScan User Manual Professional Edition. Available online, Version 1.1. <https://www.agisoft.com/>.

Aller, J., 1986. La Estructura Del Sector Meridional de Las Unidades Del Aramo y Cuenca Carbonífera Central. Servicio Publicaciones del Principado de Asturias. Consejería de Industria y Comercio, Oviedo, Spain.

Alonso, J.L., Pulgar, J.A., 1993. La Deformación Alpina En El Basamento Hercínico de La Zona Cantábrica. In: Resúmenes. XV Reunión de Xeología y Minería Do NO Peninsular, 69–71. Laboratorio Xeológico de Laxe, Laxe, Spain.

Barton, N., 1978. Suggested methods for the quantitative description of joints in rock masses. In: ISRM, International Journal of Rock Mechanics and Mining Sciences & Geomechanics Abstracts, 319–68. Great Britain: Pergamon Press.

Bellian, J.A., Kerans, C., Jennette, D.C., 2005. Digital outcrop models: applications of terrestrial scanning lidar technology in stratigraphic modeling. *J. Sediment. Res.* 75 (2), 166–176. <https://doi.org/10.2110/jsr.2005.013>.

Bieniawski, Z.T., 1989. Engineering Rock Mass Classifications: A Complete Manual for Engineers and Geologists in Mining, Civil, and Petroleum Engineering. Wiley-Interscience.

Blistan, P., Kovanič, L., Zelizňaková, V., Palková, J., 2016. Using UAV photogrammetry to document rock outcrops. *Acta Montan. Slovaca* 21 (2), 154–161.

Bonali, F.L., Tibaldi, A., Marchese, A., Fallati, L., Russo, E., Corselli, C., Savini, A., 2019. UAV-based surveying in volcano-tectonics: an example from the Iceland rift. *J. Struct. Geol.* 121 (February), 46–64. <https://doi.org/10.1016/j.jsg.2019.02.004>.

Brown, E.T., Hoek, E., 1980. Underground excavation in rock. In: Institution of Mining and Metallurgy. CRC Press, New York, USA.

Buyer, A., Aichinger, S., Schubert, W., 2020. Applying photogrammetry and semi-automated joint mapping for rock mass characterization. *Eng. Geol.* 264, 105332. <https://doi.org/10.1016/j.enggeo.2019.105332>.

October Buyer, A., Schubert, W., 2018. Joint trace detection in digital images. In: ISRM International Symposium-10th Asian Rock Mechanics Symposium. OnePetro.

Castiglioni, C.A., Rabuffetti, A.S., Chiarelli, G.P., Brambilla, G., Georgi, J., 2017. Unmanned aerial vehicle (UAV) application to the structural health assessment of large civil engineering structures. In: Papadavid, Giorgos, Hadjimitsis, Diofantos G. (Eds.), Fifth International Conference on Remote Sensing and Geoinformation of the Environment (RSCy2017), Silas Michaelides, Vincent Ambrosia, Kyriacos Themistocleous, and Gunter Schreier, 29. <https://doi.org/10.1117/12.2277921>. Paphos, Cyprus: SPIE.

Chen, L., He, Y., Chen, J., Li, Q., Zou, Q., 2016. Transforming a 3-d lidar point cloud into a 2-d dense depth map through a parameter self-adaptive framework. *IEEE Trans. Intell. Transport. Syst.* 18 (1), 165–176.

Deb, D., Hariharan, S., Rao, U.M., Ryu, C.H., 2008. Automatic detection and analysis of discontinuity geometry of rock mass from digital images. *Comput. Geosci.* 34 (2), 115–126. <https://doi.org/10.1016/j.cageo.2007.03.007>.

DeBell, L., Anderson, K., Brazier, R.E., King, N., Jones, L., 2016. Water resource management at catchment scales using lightweight UAVs: current capabilities and future perspectives. *J. Unmanned Veh. Syst.* 4 (1), 7–30. <https://doi.org/10.1139/jvus-2015-0026>.

Delormanli, A.H., Maerz, N.H., Otoo, J., 2014. Using terrestrial 3D laser scanning and optical methods to determine orientations of discontinuities at a granite quarry. *Int. J. Rock Mech. Min. Sci.* 66, 41–48. <https://doi.org/10.1016/j.ijrmm.2013.12.007>.

Dewez, T.J.B., Girardeau-Montaut, D., Allanic, C., Rohmer, J., 2016. Facets : a cloudcompare plugin to extract geological planes from unstructured 3d point clouds. *Int. Arch. Photogram. Remote. Sens. Spatial Inf. Sci. ISPRS Arch* 41, 799–804. <https://doi.org/10.5194/isprsarchives-XLI-B5-799-2016>. Available online: http://www.cloudcompare.org/doc/wiki/index.php?title=Facets_%28plugin%29.

Drews, T., Miernik, G., Anders, K., Höfle, B., Profe, J., Emmerich, A., Bechstädt, T., 2018. Validation of fracture data recognition in rock masses by automated plane detection in 3D point clouds. *Int. J. Rock Mech. Min. Sci.* 109, 19–31. <https://doi.org/10.1016/j.ijrmm.2018.06.023>.

Gallastegui, J., Pulgar, J.A., Alvarez-Marrón, J., 1997. 2-D seismic modeling of the Variscan foreland thrust and fold belt crust in NW Spain from ESCIN-1 deep seismic reflection data. *Tectonophysics* 269 (1–2), 21–32. [https://doi.org/10.1016/S0040-1951\(96\)00166-7](https://doi.org/10.1016/S0040-1951(96)00166-7).

García-López, S., Ruiz-Ortiz, V., Barbero, L., Sánchez-Bellón, A., 2018. Contribution of the UAS to the determination of the water budget in a coastal wetland: a case study in the natural park of the Bay of Cádiz (SW Spain). *Eur. J. Remote Sens.* 51 (1), 965–977. <https://doi.org/10.1080/22797254.2018.1522602>.

Giordan, D., Manconi, A., Tannant, D.D., Allasia, P., 2015. UAV: low-cost remote sensing for high-resolution investigation of landslides. In: International Geoscience and Remote Sensing Symposium (IGARSS) 2015-November. <https://doi.org/10.1109/IGARSS.2015.7327042>, 5344–47.

Giordan, D., Adams, M.S., Aicardi, I., Alicandro, M., Allasia, P., Baldo, M., et al., 2020. The use of unmanned aerial vehicles (UAVs) for engineering geology applications. *Bull. Eng. Geol. Environ.* 79 (7), 3437–3481. <https://doi.org/10.1007/s10064-020-01766-2>.

Girardeau-Montaut, D., 2016. CloudCompare. Available online: <https://www.danielgm.net/cc/> <https://github.com/cloudcompare/cloudcompare>.

Guo, J., Liu, Y., Wu, L., Liu, S., Yang, T., Zhu, W., Zhang, Z., 2019. A geometry-and texture-based automatic discontinuity trace extraction method for rock mass point cloud. *Int. J. Rock Mech. Min. Sci.* 124, 104132.

Hack, R., Price, D., Rengers, N., 2003. A new approach to rock slope stability - a probability classification (SSPC). *Bull. Eng. Geol. Environ.* 62 (2), 167–184. <https://doi.org/10.1007/s10064-002-0155-4>.

Herrero Fernández, M.J., Escavy Fernández, J.I., Insúa Arévalo, J.M., De la Horra del Barco, R., Sánchez Moya, Y., Sopena Ortega, A., Álvarez Gómez, J.A., López Acevedo, F.J., Jiménez Molina, D., Trigos Luque, L., Fregenal Martínez, M.A., Martínez Díaz, J.J., Menéndez-Pidal de Navascués, I., Rey Samper, J.J., Sanz Pérez, E., Varas Muriel, M.J., Sanz de Ojeda, J., Sanz de Ojeda, P., Arribas Mocoora, J., Álvarez Sierra, M.A., Uribelarra del Val, D., 2019. RPAS (Remotely Piloted Aircraft Systems) para la elaboración de salidas de campo virtuales como recursos docentes “flipped classroom” para Grados relacionados con Ciencias de la Tierra. <https://eprints.ucm.es/id/eprint/57600/>.

Hudson, J.A., 2001. Engineering Rock Mechanics: Part 2: Illustrative Worked Examples. Elsevier Science, Oxford, UK.

James, M.R., Robson, S., 2012. Straightforward reconstruction of 3D surfaces and topography with a camera: accuracy and geoscience application. *J. Geophys. Res.: Earth Surf.* 117 (3), 1–17. <https://doi.org/10.1029/2011JF002289>.

Jianqin, C., Zhu, H., Li, X., 2016. Automatic extraction of discontinuity orientation from rock mass surface 3D point cloud. *Comput. Geosci.* 95, 8–31. <https://doi.org/10.1016/j.cageo.2016.06.015>.

Jones, D.A., Hansen, A.J., Bly, K., Doherty, K., Verschuyt, J.K., Paugh, J.I., Carle, R., Story, S.J., 2009. Monitoring land use and cover around parks: a conceptual approach. *Rem. Sens. Environ.* 113 (7), 1346–1356. <https://doi.org/10.1016/j.rse.2008.08.018>.

Jordá Berdehore, L., Riquelme, A., Cano, M., Tomás, R., 2017. Comparing manual and remote sensing field discontinuity collection used in kinematic stability assessment of failed rock slopes. *Int. J. Rock Mech. Min. Sci.* 97 (June), 24–32. <https://doi.org/10.1016/j.ijrmm.2017.06.004>.

Julivert, M., 1978. Hercynian orogeny and carboniferous palaeogeography in northwestern Spain; a model of deformation-sedimentation relationships. *Z. Dtsch. Geol. Ges.* 129 (2), 565–592.

- Kemeny, J., Turner, K., Norton, B., 2006. LIDAR for rock mass characterization: hardware, software, accuracy, and best practices. In: *Laser and Photogrammetric Methods for Rock Face Characterization Workshop*, pp. 49–62 (Golden, Colorado).
- Kong, D., Saroglou, C., Wu, F., Sha, P., Li, B., 2021. Development and application of UAV-SfM photogrammetry for quantitative characterization of rock mass discontinuities. *Int. J. Rock Mech. Min. Sci.* 141, 104729 <https://doi.org/10.1016/j.ijrmms.2021.104729>.
- Labourdette, R., Jones, R.R., 2007. Characterization of fluvial architectural elements using a three-dimensional outcrop data set: Escanilla braided system, south-central pyrenees, Spain. *Geosphere* 3 (6), 422–434. <https://doi.org/10.1130/GES00087.1>.
- Lato, M., Kemeny, J., Harrap, R.M., Bevan, G., 2013. Rock bench: establishing a common repository and standards for assessing rockmass characteristics using LiDAR and photogrammetry. *Comput. Geosci.* 50, 106–114. <https://doi.org/10.1016/j.cageo.2012.06.014>.
- Li, X., Chen, J., Zhu, H., 2016. A new method for automated discontinuity trace mapping on rock mass 3D surface model. *Comput. Geosci.* 89, 118–131.
- Lotze, F., 1945. Zur gliederung der Varisziden der iberischen meseta. *Geotekt. Forsch.* 6, 78–92.
- Madden, M., Jordan, T., Bernardes, S., Cotton, D.L., O'Hare, N., Pasqua, A., 2015. Unmanned aerial systems and structure from motion revolutionize wetlands mapping. In: Tiner, Ralph W., Lang, Megan W., Klemas, Victor V. (Eds.), *Remote Sensing of Wetlands: Applications and Advances*. CRC Press, pp. 195–214.
- Maerz, N.H., Youssef, A.M., Otoo, J.N., Kassebaum, T.J., Duan, Y.E., 2013. A simple method for measuring discontinuity orientations from terrestrial LIDAR data. *Environ. Eng. Geosci.* 19 (2), 185–194.
- Mah, J., Samson, C., McKinnon, S.D., 2011. 3D laser imaging for joint orientation analysis. *Int. J. Rock Mech. Min. Sci.* 48 (6), 932–941. <https://doi.org/10.1016/j.ijrmms.2011.04.010>.
- Marcos, A., Pulgar, J.A., 1982. An approach to the tectonostratigraphic evolution of the cantabrian foreland thrust and fold belt, Hercynian Cordillera of NW Spain. *Neues Jahrb. Geol. Palaeontol. Abh.* 163 (2), 256–260.
- Menegoni, N., Giordan, D., Perotti, C., Tannant, D.D., 2019. Detection and geometric characterization of rock mass discontinuities using a 3D high-resolution digital outcrop model generated from RPAS imagery—Ormea rock slope. *Ital. Engol. Geol.* 252, 145–163. <https://doi.org/10.1016/j.enggeo.2019.02.028>.
- Nesbit, P.R., Boulding, A.D., Hugenholtz, C.D., Durkin, P.R., Hubbard, S.M., 2020. Visualization and sharing of 3D digital outcrop models to promote open science. *GSA Today (Geol. Soc. Am.)* 30 (6). <https://doi.org/10.1130/GSATG425GW.1>.
- Ouédraogo, M.M., Degré, A., Debouche, C., Lisein, J., 2014. The evaluation of unmanned aerial system-based photogrammetry and terrestrial laser scanning to generate DEMs of agricultural watersheds. *Geomorphology* 214, 339–355. <https://doi.org/10.1016/j.geomorph.2014.02.016>.
- August Pack, G., Kieffer, D.S., Metzler, I., Liu, Q., 2021. Approaches for the digital measurement of rock mass discontinuities, 1. In: *IOP Conference Series: Earth and Environmental Science*, vol. 833. IOP Publishing, 012059.
- Pantelidis, L., 2009. Rock slope stability assessment through rock mass classification systems. *Int. J. Rock Mech. Min. Sci.* 46 (2), 315–325. <https://doi.org/10.1016/j.ijrmms.2008.06.003>.
- Pix 4D mapper, 2018. Available from: <https://www.pix4d.com/es/>. . on June 2018.
- Pérez-Estaún, A., Bastida, F., Alonso, J.L., Marquínez, J., Aller, J., Alvarez-Marrón, J., Marcos, A., Pulgar, J.A., 1988. A thin-skinned tectonics model for an arcuate fold and thrust belt; the Cantabrian Zone (Variscan iberico-Armorican arc). *Tectonics* 7 (3), 517–537.
- Raeva, P.L., Filipova, S.L., Filipov, D.G., 2016. Volume computation of a stockpile - a study case comparing GPS and uav measurements in an open pit quarry. *Int. Arch. Photogram. Remote. Sens. Spatial Inf. Sci. ISPRS Arch* 2016, 999–1004. <https://doi.org/10.5194/isprsarchives-XLI-B1-999-2016>.
- Rencher, A., 2012. *Methods of Multivariate Analysis*, second ed. John Wiley & Sons Ltd, New York, USA.
- Riquelme, A.J., Abellán, A., Tomás, R., Jaboyedoff, M., 2014. A new approach for semi-automatic rock mass joints recognition from 3D point clouds. *Comput. Geosci.* 68, 38–52. <https://doi.org/10.1016/j.cageo.2014.03.014>. Available online: <https://github.com/adriquiriquelme/DSE>.
- Riquelme, A.J., Abellán, A., Tomás, R., 2015. Discontinuity spacing analysis in rock masses using 3D point clouds. *Eng. Geol.* 19, 185–195. <https://doi.org/10.1016/j.enggeo.2015.06.009>.
- Riquelme, A., Tomás, R., Cano, M., Abellán, A., 2016. Using open-source software for extracting geomechanical parameters of a rock mass from 3D point clouds: discontinuity set extractor and SMRTTool. In: *ISRM International Symposium - EUROCK 2016*. <https://doi.org/10.1201/9781315388502-190>. October, 1091–96.
- Romana, M., 1985. New adjustment ratings for application of Bieniawski classification to slopes. In: *Proceedings of the International Symposium on Role of Rock Mechanics. Zacatecas, Mexico*, pp. 49–53.
- Sánchez Moya, Y., Jiménez Molina, D., Álvarez Gómez, J.A., Martínez Díaz, J.J., Insua Arevalo, J.M., Fregenal Martínez, M.A., Herrero Fernández, M.J., Varas Muriel, M.J., Morellón Marteles, M., De La Horra Del Barco, R., Sanz Pérez, E., Escavy Fernández, J.I., Sopena Ortega, A., Menéndez-Pidal De Navascues, I., Trigos Luque, L., Rey Samper, J.J., López Acevedo, F.J., Sanz De Ojeda, P., Sanz De Ojeda, J., 2020. Uso de RPAS (Remotely Piloted Aircraft System) Para La Docencia y Divulgación de Las Ciencias de La Tierra. <https://eprints.ucm.es/id/eprint/61148/>.
- Sánchez, V., Vindel, E., Martín-Crespo, T., Corbella, M., Cardellach, E., Banks, D., 2009. Sources and composition of fluids associated with fluorite deposits of asturias (N Spain). *Geofluids* 9 (4), 338–355. <https://doi.org/10.1111/j.1468-8123.2009.00259.x>.
- Siebert, S., Teizer, J., 2014. Mobile 3D mapping for surveying earthwork projects using an unmanned aerial vehicle (UAV) system. *Autom. Construct.* 41, 1–14. <https://doi.org/10.1016/j.autcon.2014.01.004>.
- Silverman, B., 1986. *Density Estimation for Statistics and Data Analysis*. Chapman & Hall/CRC Monographs on Statistics & Applied Probability, Taylor & Francis, New York, USA.
- Sketchfab, 2020. Available from: <https://sketchfab.com/>. May 2020.
- Slob, S., Van Knapen, B., Hack, R., Turner, K., Kemeny, J., 2005. Method for automated discontinuity analysis of rock slopes with three-dimensional laser scanning. *Transport. Res. Rec.* 187–194. <https://doi.org/10.3141/1913-18>, 1913.
- Sturzenegger, M., Stead, D., 2009. Close-range terrestrial digital photogrammetry and terrestrial laser scanning for discontinuity characterization on rock cuts. *Eng. Geol.* 106 (3–4), 163–182. <https://doi.org/10.1016/j.enggeo.2009.03.004>.
- Tomás, R., Cuenca, A., Cano, M., García-Barba, J., 2012. A graphical approach for slope mass rating (SMR). *Eng. Geol.* 124 (1), 67–76. <https://doi.org/10.1016/j.enggeo.2011.10.004>.
- Tu, Y.H., Johansen, K., Aragon, B., Stutsel, B.M., Ángel, Y., Camargo, O.A.L., McCabe, M.F., 2021. Combining Nadir, Oblique, and Façade imagery enhances reconstruction of rock formations using unmanned aerial vehicles. *IEEE Trans. Geosci. Rem. Sens.* 59 (12), 9987–9999.
- Tziavou, O., Pytharouli, S., Souter, J., 2018. Unmanned aerial vehicle (UAV) based mapping in engineering geological surveys: considerations for optimum results. *Eng. Geol.* 232, 12–21. <https://doi.org/10.1016/j.enggeo.2017.11.004>.
- Vasuki, Y., Holden, E.J., Kovesi, P., Micklethwaite, S., 2014. Semi-automatic mapping of geological structures using UAV-based photogrammetric data: an image analysis approach. *Comput. Geosci.* 69, 22–32. <https://doi.org/10.1016/j.cageo.2014.04.012>.
- Verhoeven, G., 2011. Taking computer vision aloft - archaeological three-dimensional reconstructions from aerial photographs with photostan. *Archaeol. Prospect.* 18 (1), 67–73. <https://doi.org/10.1002/arp.399>.
- Wang, L.G., Yamashita, S., Sugimoto, F., Pan, C., Tan, G., 2003. A methodology for predicting the in situ size and shape distribution of rock blocks. *Rock Mech. Rock Eng.* 36 (2), 121–142. <https://doi.org/10.1007/s00603-002-0039-8>.
- Wang, X., Silva, P., Bello, N.M., Singh, D., Evers, B., Mondal, S., Espinosa, F.P., Singh, R.P., Poland, J., 2020. Improved accuracy of high-throughput phenotyping from unmanned aerial systems by extracting traits directly from orthorectified images. *Front. Plant Sci.* 11, 1–14. <https://doi.org/10.3389/fpls.2020.587093>.
- Westoby, M.J., Brasington, J., Glasser, N.F., Hambrey, M.J., Reynolds, J.M., 2012. Structure-from-Motion photogrammetry: a low-cost, effective tool for geosience applications. *Geomorphology* 179, 300–314. <https://doi.org/10.1016/j.geomorph.2012.08.021>.
- Yusoff, A.R., Darwin, N., Majid, Z., Ariff, M.F.M., Idris, K.M., 2018. Comprehensive analysis of flying altitude for high resolution slope mapping using UAV technology. *Int. Arch. Photogram. Remote. Sens. Spatial Inf. Sci. ISPRS Arch* 42 (3W4), 583–589. <https://doi.org/10.5194/isprs-archives-XLII-3-W4-583-2018>.